

Exit-Channel Suppression in Statistical Reaction Theory

G.F. Bertsch¹ and T. Kawano²

¹*Department of Physics and Institute of Nuclear Theory,
University of Washington, Seattle, Washington 98915, USA*

²*Theoretical Division, Los Alamos National Laboratory,
Los Alamos, New Mexico 87545, USA*

Abstract

Statistical reaction theories such as Hauser-Feshbach assume that branching ratios follow Bohr's compound nucleus hypothesis by factorizing into independent probabilities for different channels. Corrections to the factorization hypothesis are known in both nuclear theory and quantum transport theory, particularly an enhanced memory of the entrance channel. We apply the Gaussian orthogonal ensemble to study a complementary suppression of exit channel branching ratios. The combined effect of the width fluctuation and the limitation on the transmission coefficient can provide a lower bound on the number of exit channels. The bound is demonstrated for the branching ratio in neutron-induced reactions on a ^{235}U target.

Introduction. Statistical approximations are extremely useful in nuclear physics, particularly in reaction theory. Examples are the Hauser-Feshbach and Weisskopf-Ewing formulas for reaction cross sections [1–3]. The underlying assumption of both is the factorizability of the cross section σ_{ab} from one channel to another as $\sigma_{ab} \sim \Gamma_a \Gamma_b$, where Γ_i is the average decay width through a channel. The factorization follows from Bohr’s compound nucleus hypothesis [4], that the decay of a heavy nucleus has no memory of how it was formed. However, factorization is only justified when the reaction takes place through discrete resonances and there are many channels contributing to each decay mode. Otherwise, the fluctuations in the widths of the resonance gives rise to the well-known “width fluctuation correction” (WFC) to the statistical models [5], most prominently as the “elastic enhancement factor.” There is now an extensive literature on the subject cited in Refs. [6] and [7]. Similar effects in electron propagation through mesoscopic conductors are known as the “weak localization correction” and the “dephasing” effect [8, Sect. IV.C and IV.E].

While the nuclear correction is best known as an entrance channel effect, it can also be present in exit channels if the reaction branching ratios highly favor a decay mode with large fluctuations [9]. In this work we show that such situations can lead to effects large enough to provide bounds on the number of channels in the decay mode, even though the measurements are on averaged quantities and not on their fluctuations. This study was motivated in part by the quest for a theory of fission dynamics based on nucleon-nucleon interactions. That requires an understanding not only of the distribution of the fission channels but their coupling matrix elements to the other states.

The GOE statistical model. The factorization hypothesis and other statistical aspects of reaction theory can be tested theoretically by models that consider ensembles of Hamiltonians that mix the constituent configurations. The Gaussian orthogonal ensemble (GOE) has been especially successful in this regard [6, 7]. The reaction theory is expressed in the matrix equations

$$K = \pi \gamma^T \frac{1}{E - H} \gamma \quad (1)$$

$$S = \frac{1 - iK}{1 + iK} \quad (2)$$

giving for the non-elastic cross sections [10]

$$\sigma_{nf} = \frac{\pi}{k_n^2} \sum_{c \in f} |S_{nc}|^2 . \quad (3)$$

In Eq. (1) K is a matrix of dimension $N^{ch} \times N^{ch}$, where N^{ch} is the number of reaction channels in the model. H is the $N_\mu \times N_\mu$ Hamiltonian matrix for the N_μ internal states in the model. The internal states are connected to the channels by the $N^{ch} \times N_\mu$ reduced-width matrix γ . Eq. (2) relates the K -matrix to the familiar S -matrix of scattering theory. There is an additional overall phase factor in Eq. (2) which plays no role in the reaction cross sections. In Eq. (3) n is the entrance channel, f is a set of exit channels that are grouped together in an experimental cross section, and c are the individual channels. The cross section depends explicitly on the entrance channel energy E_n via the neutron wave-number $k_n = \sqrt{2E_n M_n}$, with M_n the reduced mass.

In the GOE statistical model, the Hamiltonian H is sampled from the distribution [11]

$$H_{\mu,\mu'} = H_{\mu',\mu} = v_{\mu,\mu'} (1 + \delta_{\mu,\mu'})^{1/2}, \quad (4)$$

where $\mu \geq \mu'$ and $v_{\mu,\mu'}$ is a Gaussian-distributed random variable. The ensemble is completely specified by N_μ and the r.m.s. Hamiltonian matrix element $\langle v^2 \rangle^{1/2}$. Here we shall characterize the GOE ensemble by D , the average level spacing in the middle of the distribution. The spacing is related to the matrix elements by $D = \pi \langle v^2 \rangle^{1/2} N_\mu^{-1/2}$. The γ matrix associated with a GOE Hamiltonian can be assumed to have a diagonal structure of the form $\gamma|_{\mu,c} = \gamma_c \delta_{\mu,c}$. In this work, we also make the simplifying assumption that the γ_c are equal for all channels within a given decay mode f . When the matrix is transformed to the basis diagonalizing the GOE Hamiltonian, the amplitudes will be distributed over eigenstates according to the Porter-Thomas distribution [12] with a number of degrees of freedom equal to the number of channels N_f . It will be convenient to define an effective K -matrix decay rate for the different modes Γ_f^K as

$$\Gamma_f^K = \frac{2\pi}{N_\mu} \sum_{c \in f} \gamma_c^2. \quad (5)$$

If all the Γ_f^K are small compared to D , the average S -matrix decay widths satisfy

$$\Gamma_f \approx \Gamma_f^K. \quad (6)$$

Note also that $N_n^{ch} = 1$ for the entrance channel; its reduced width controls the total reaction cross section [13].

The calculations reported below were carried out with codes that constructed the GOE distribution by Monte Carlo sampling of H and applying Eqs. (1-3). The codes and input data are provided in the Supplementary Material [14].

Application to the branching ratio $^{235}\text{U}(n,f)/^{235}\text{U}(n,\gamma)$. Here we show by a physical example that cross-section branching ratios that heavily favor some particular exit channel can be severely suppressed. The behavior follows from the GOE statistical model as formulated in the last section and is thus universal. Our example is the neutron-induced reactions on ^{235}U . For neutron energies below ~ 10 keV the predominant reactions are in the s -wave leading to capture by gamma emission or fission. An important quantity is α^{-1} , the ratio of the fission cross section σ_F to capture cross section σ_{cap} , $\alpha^{-1} = \sigma_F/\sigma_{cap}$. It varies in the range $\alpha^{-1} \sim 2$ -3 in the 1 - 15 keV energy range[15]. The capture widths can assumed to be constant over this energy interval, since the interval is very small compared to the excitation energy (~ 6.5 MeV) and capture takes place through many channels. The same is true of the level density, since the effective temperature is of the order of 0.5 MeV. Table I gives approximate values of measured D and Γ_{cap} which will be used to determine the parameters of the K -matrix [16] We will examine the cross section at $E_n = 10$ keV; the experimental

TABLE I: Experimental observables for neutron-induced reactions on ^{235}U . The cross section data is at a neutron bombarding energy $E_n = 10$ keV. The last two entry are the ratio of cross sections, show the range of the ratios as well as the value at 10 keV.

Observable	Value	Source
D	0.45 ± 0.05 eV	[17, 23]
Γ_{cap}	38 ± 3 meV	[17]
σ_{cap}	1.05 ± 0.07 b	[18, 19]
σ_F	2.96 ± 0.06 b	[18, 19]
$\alpha^{-1}(10)$	2.8 ± 0.2	[19, 20]
$\alpha^{-1}(1 - 15)$	2-3.1	[18]

values averaged over a 1 keV are also given in Table I.

The K -matrix reduced-width parameters are determined as follows. The capture width is small compared to D and many channels contribute so we can safely apply Eq. (6); the equivalent Γ_{cap} is shown in Table II. The coupling to the entrance channel depends on E_n and is usually parameterized by the strength function S_0 as

$$\frac{\langle \Gamma_n \rangle}{D} = S_0 E^{1/2}. \quad (7)$$

From total cross sections one finds $S_0 \approx 1 \pm 0.1 \times 10^{-4} \text{ eV}^{-1/2}$ [22, 23],[24, Fig. 47] and we use that value to determine the entry in Table II. We note that this value is consistent with the coupled-channel analysis of Ref. [25]. For the fission reduced width, we first make the factorization (Hauser-Feshbach) approximation and assume that the nominal decay widths scale with the cross sections, i.e. $\Gamma_F^K/\Gamma_{cap}^K = \sigma_F/\sigma_{cap}$.

TABLE II: K -matrix parameters (eV) describing observed cross sections at $E_n = 10 \text{ keV}$ in Hauser-Feshbach theory and assuming $\Gamma \ll D$. We have also include the parameters from the ENDF/B-VII.1 evaluation.

	Γ_{cap}^K	Γ_F^K	Γ_n^K
this work	0.038 ± 3	0.105 ± 0.01	0.010 ± 0.001
ENDF	0.039	0.289	0.0097

The number of channels and states in the K -matrix are still to be specified. As presented, the model is independent of the number of states as long as that number is large. We shall take $N_\mu = 50 - 100$. The capture channels do not show large fluctuations and one can therefore assume that $N_{cap}^{ch} \gg 1$; we take $N_{cap}^{ch} = 10$ in our modeling. The number of fission channels is not well known [26] and we consider two possibilities: model A with one fission channel and model B with five fission channels.

With all parameters now specified in the GOE K -matrix, we can compute the average cross sections and branching ratios. These are shown in Table III. In model A, one sees

TABLE III: Average reaction cross sections at $E_n = 10 \text{ keV}$, comparing models A and B with experiment. The uncertainties on the calculated values are the r.m.s. sample-to-sample fluctuations associated with the random matrix ensemble of the internal states, taking a 1 keV averaging interval. We have also included in the table the impact on the elastic scattering S -matrix.

	N_F^{ch}	σ_F (b)	σ_{cap} (b)	α^{-1}	$ S_{nn} ^2$
Exp.		2.96 ± 0.21	1.06 ± 0.07	2.8	
A	1	1.66 ± 0.05	1.39 ± 0.05	1.20 ± 0.07	0.954
B	5	2.28 ± 0.10	1.00 ± 0.06	2.3 ± 0.11	0.950

TABLE IV: Average fission widths Γ_F^K required to reproduce the observed cross-section ratio $\alpha^{-1} = 2.8 \pm 0.2$ in various models. HW: Hauser-Feshbach; HW/WFC; Hauser-Feshbach with width fluctuation correction from Eq. (8); KtoS: Eqs. (1-3). The uncertainty of the observed α^{-1} is propagated through the models to give the uncertainty bars in the table. Units are eV.

Model	N_{cap}^{ch}	N_F^{ch}	HW	HW/WFC	KtoS
A	10	1	0.107 ± 0.008	0.46 ± 0.06	none
B	10	5	0.107 ± 0.008	0.13 ± 0.01	0.136 ± 0.01

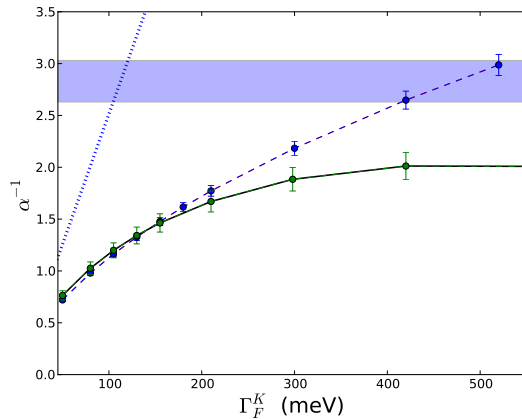


FIG. 1: Cross section ratio $\alpha^{-1} = \langle \sigma_F \rangle / \langle \sigma_{cap} \rangle$ as a function of average fission width Γ_F^K assuming a single fission channel. Solid line: Eq. (1-3). Dotted line: Hauser-Feshbach approximation, i.e. $\alpha^{-1} = \Gamma_F^K / \Gamma_{cap}^K$. Dashed line: Hauser-Feshbach including the WFC correction, Eq. (8). Blue band: experimental range, taking uncertainty from Table I. Widths are the statistical errors associated with the 1 keV cross-section averaging interval.

an enhancement of the capture cross section and a corresponding suppression of the fission cross section. Clearly factorization is violated.

Let us see if we can reproduce the experimental branching ratio simply by increasing the fission width, but keeping only a single channel. Taking the width as a free parameter, we obtain the branching ratios shown as the solid line in Fig. 1. Also, we show in Table IV the values of Γ_F^K required to fit the observed branching ratio. Model A saturates at $\alpha^{-1} \sim 2.0$; there is no reasonable value of Γ_F^K that can reproduce experiment. Thus, we can exclude

fission models having only a single channel, based solely on average cross section data. Of course, the fluctuation in cross-section ratios also carries information on the number of channels and is the basis of previous estimates that the effect channel count is of the order of a few. Finally, one can see from the second line of Table IV that model B can fit the data taking the decay with close to the Hauser-Feshbach value.

Discussion. The exit channel suppression comes about by two mechanisms that can be understood as follows. The part coming from Porter-Thomas fluctuations can be analyzed at the level of the K -matrix: assuming isolated resonances, the branching ratio can be calculated as in Ref. [22],

$$\alpha^{-1} = \left\langle \frac{\Gamma_F^K}{\sum_f \Gamma_f^K} \right\rangle \bigg/ \left\langle \frac{\Gamma_{cap}^K}{\sum_f \Gamma_f^K} \right\rangle. \quad (8)$$

The results are shown as the dashed line in Fig. 1. For $\Gamma_F^K = 0.105$ eV, Eq. (8) gives a WFC factor of 0.43, close to that of the full S -matrix treatment. However, to explain the observed α^{-1} , we have to go to much larger fission width, $\Gamma_F^K \approx 0.46$ eV, as may be seen in Table IV. At that width the WFC factor is 0.23 in the HF/WFC treatment and 0.16 in the full S -matrix treatment. Increasing Γ_F^K further does not raise the S -matrix value significantly.

We attribute the additional suppression in the S -matrix treatment to the constraint on statistical decay rates W_f imposed by the Bohr-Wheeler formula [27]

$$W_f = \Gamma_f = \frac{1}{2\pi} DT, \quad (9)$$

where T is the transmission coefficient of the channel. General considerations of detailed balance require $T \leq 1$. The nominal fission width in the K -matrix reduced width is close to the bound, so it is not unexpected that there is a further suppression in the S -matrix.

Conclusion. We have demonstrated that branching ratios can be a useful observable in the study of fission dynamics near threshold. Namely, effects not included in the Hauser-Theory can severely constrain the number of exit channels. In the example presented here, the energy of the fissioning nucleus is above the fission barrier. It might be of interest to apply the analysis to below-barrier fission as well [28]. There one sees sharp peaks in the fission cross section, ascribed to individual states along the fission path. These states act as fission channels with $N_F^{ch} = 1$ in the K -matrix modeling.

We confirmed the generality of our conclusion by exploring a variety of channel number and transmission combinations. Several examples are provided in Supplemental Material.

The repository also contains the main code implementing Eq. (1-4) and the script to compute the branching ratio and its uncertainty.

Acknowledgments. The authors thank Y. Alhassid for discussing connections to quantum transport theory and D. Brown for providing archived experimental data. We also thank W. Nazarewicz, R. Capote, and H.A. Weidenmüller for very helpful comments on an earlier version of this manuscript.

-
- [1] J.E. Escher and F.S. Dietrich, Phys. Rev. C **74** 054601 (2006).
 - [2] V.F. Weisskopf and D.H. Ewing, Phys. Rev. **57** 472 (1940).
 - [3] W. Hauser and H. Feshbach, Phys. Rev. **87** 366 (1952).
 - [4] N. Bohr, Nature **137** 344 (1936).
 - [5] P.A. Moldauer, Phys. Rev. C **11** 426 (1975).
 - [6] G.E. Mitchell, A. Richter, and H.A. Weidenmüller, Rev. Mod. Phys. **82** 2845 (2010).
 - [7] T. Kawano, P. Talou and H.A. Weidenmüller, Phys. Rev. C **92** 044617 (2015).
 - [8] Y. Alhassid, Rev. Mod. Phys. **72** 895 (2000).
 - [9] P. Moldauer, Phys. Rev. C **14** 764 (1976)
 - [10] There is also an angular-momentum statistical factor in Eq. (3) that we ignore here. See also footnote [13].
 - [11] M.L. Mehta, *Random Matrices*, 3rd Edition, Academic Press (2004).
 - [12] C.E. Porter and G.E. Thomas, Phys. Rev. **104** 483 (1956).
 - [13] There are in fact two independent entrance channels distinguished by total angular momentum and the actual resonance spacing is $D \approx 0.45$ [17]. The spacing within each channel is about twice D_0 [22]. We assume they behave similarly.
 - [14] The codes used for the calculations reported here are available upon request to `bertsch@uw.edu`.
 - [15] Determined by ratio of averaged ENDF cross sections over a 1 keV averaging interval.
 - [16] D in this table includes the two independent entrance channels. The input value for the individual entrance channels calculated here is about twice as large.
 - [17] R. Capote *et al.*, Nuclear Data Sheets **110** 3107, (2009).
 - [18] M.B. Chadwick *et al.*, Nuclear Data Sheets **112** 2887, (2011).

- [19] Uncertainty estimates from F. Corvi, et al., Argonne National Laboratory Report ANL-83-4 (1982), reported in INDC (EUR) 015/G Table 1.1.
- [20] The uncertainty of the alpha ratio is much larger at higher energies due to inconsistencies in the reported cross sections. See Ref. [21].
- [21] P. Talou, et al., Nuclear Data Sheets **112** 3054 (2011).
- [22] M.S. Moore, J.D. Moses, G.A. Keyworth, J.W. Dobbs and N.W. Hill, Phys. Rev. C **18** 1328 (1978), Table IV.
- [23] S. Mughabghab, *Neutron Cross Sections* Vol. 1B (Academic Press, 1984).
- [24] A.J. Koning and J.P. Delaroche, Nucl. Phys. A **713** 231 (2003).
- [25] E. Sh. Soukhovitskii, R. Capote, J. M. Quesada, S. Chiba Phys. Rev. C **72**, 024604 (2005).
- [26] M. Sin, R. Capote, M. W. Herman, and A. Trkov, Phys. Rev. C **93** 034605 (2016)
- [27] N. Bohr and J.A. Wheeler, Phys. Rev. **56** 426 (1939).
- [28] O. Bouland, J.E. Lynn, and P. Talou, Phys. Rev. C **88** 054612 (2013).
- [29] The errors are estimated to be 7% based on the data of [30].
- [30] R.B. Perez, et al., Nuclear Science and Engineering **55** 203 (1974).